

## Theoretical Aspects of Methanol Carbonylation on Copper-Containing Zeolites

A. A. Rybakov<sup>a</sup>, I. A. Bryukhanov<sup>b, c</sup>, A. V. Larin<sup>a</sup>, and G. M. Zhidomirov<sup>a, d, e</sup>

<sup>a</sup> Faculty of Chemistry, Moscow State University, Moscow, Russia

<sup>b</sup> Faculty of Mechanics and Mathematics, Moscow State University, Moscow, Russia

<sup>c</sup> Research Institute of Mechanics, Moscow State University, Moscow, Russia

<sup>d</sup> Borekov Institute of Catalysis, Siberian Branch, Russian Academy of Sciences, Novosibirsk, Russia

<sup>e</sup> Zelinsky Institute of Organic Chemistry, Russian Academy of Sciences, Moscow

e-mail: nasgo@yandex.ru

Received November 16, 2015

**Abstract**—The experimental data have been considered to match the theoretical mechanisms proposed previously to describe processes of oxidative carbonylation of methanol on copper-containing catalysts. The schemes examined cover methoxy intermediates, carbomethoxy intermediates, carbonates, and Cu(OCH<sub>3</sub>)<sub>2</sub>Cu binuclear clusters. The attack of the first methanol molecule on copper carbonate has been simulated in terms of the isolated cluster (8R) model with periodic boundary conditions (on CuMOR zeolite), and parameters of the individual steps involving description of the transition states have been evaluated.

**Keywords:** methanol carbonylation, carbonates, zeolites, copper-containing catalysts, DFT

**DOI:** 10.1134/S0965544116030129

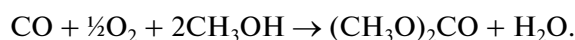
Environmental problems of application of phosgene in the existing technologies for production of polyurethanes, polycarbonates, and dimethyl carbonate (DMC) necessitate the search for new methods of DMC synthesis. This modern “green” reagent and solvent could replace both phosgene as the carbonylating agent and dimethyl sulfate in methylation of phenols and naphthols. Dimethyl carbonate is also used as a fuel additive that enhances the octane number.

Liquid-phase synthesis of DMC from methanol and phosgene in copper salt solutions is accompanied by corrosion and deactivation of the reactants. As an alternative to the liquid-phase synthesis of DMC, the use of zeolites can turn to be a more promising process. Copper forms of zeolites can be used for binding CO as DMC via a sequence of oxidative carbonylation reactions [1–4]. Reactions in a homogeneous (copper halides with different ligands [1–6]) or a heterogeneous (CuX [7, 8], CuZSM-5 [8], CuY [9–11], CuY/beta-SiC [12] or on carbon-supported CuCl [9]) medium lead to comparable yields of DMC and selectivity without loss of activity in the case of heterogeneous catalysis.

The synthesis of DMC is known to have been carried out on the copper forms of zeolites ZSM-5 [8], X [7], Y [9], and MOR [13]. A more complete survey of supports for heterogeneous catalysis and ligands for homogeneous catalysis is presented in reviews [14–16]. Considering the variety of ligands for Cu<sup>+</sup> cations in oxidative carbonylation reactions, Raab et al. [6]

pointed out the capability of *N*-methylimidazole, which stimulates the capture of molecular oxygen, and associated the oxidation of CO to DMC on the copper form of zeolite with the formation of binuclear clusters Cu<sub>2</sub>O<sub>2</sub> of different geometries. Interaction of these systems with a Cu<sub>2</sub>O<sub>2</sub> fragment in a homogeneous medium was reviewed in [17, 18]. At the same time, the conversion of both methanol and heavier alcohols remains low, on the order of 10%, in the heterogeneous synthesis [9, 10] and calls for further investigation to improve it.

In studies on liquid-phase processes, four carbonylation mechanisms have been suggested: the formation of methoxy intermediates (M intermediates) [1, 2], carbomethoxy intermediates (CM intermediates) (both versions can involve one or two copper atoms, i.e., be a one- or two-center mechanism) [3, 4], and monomethyl carbonate (MMC) [10] and a CO attack at the complex Cu(OCH<sub>3</sub>)<sub>2</sub>Cu with two copper atoms [2]. The classification of the mechanisms is associated with both the type of intermediate and the number of cations involved in the reaction; i.e., the features that go beyond the conventional overall equation of the reaction:



One of the first DMC synthesis schemes including byproducts (dimethoxymethane (DMM), methyl formate, formaldehyde) was suggested by King [9] with allowance for the conclusions made by Romano et al.

[4], who in turn relied on the data obtained by Koch et al. [3]. The King's assumption about the formation of a new type of CM intermediate was based on the finding that the C=O vibration frequency shifts from  $1664\text{ cm}^{-1}$  (presumably in MMC) to  $1690\text{ cm}^{-1}$  (presumably in the CM intermediate) [9]. More specifically, the frequencies  $1694$ ,  $1665$ ,  $1348$ , and  $1333\text{ cm}^{-1}$  [9] were assigned to the CM intermediate. They are close to the frequencies of  $1690$ ,  $1664$ ,  $1353$  (or  $1348$ ), and  $1333\text{ cm}^{-1}$  reported later [10]. King [9] showed that the limiting step is the insertion of CO and described  $\text{Cu}^{+2}$  as an inactive form. The latter conclusion was later challenged in [11]. Unlike other investigators [4, 7], King did not discuss (e.g., based on kinetic analysis data, as in [7]) how many centers (one or two  $\text{Cu}^+$  cations) are involved in individual steps, whereas Romano et al. [4] supposed all the CM formation steps to occur on two cations. Note that in the aforementioned study [4] devoted to the liquid-phase process on CuCl, the formation of DMC was found to follow the first-order rate law in  $\text{O}_2$  pressure, which conforms to Eq. (1). Later, this order was not confirmed for the reactions on zeolites, such as CuY, CuZSM-5, and CuMOR [13].

Anderson and Root [7] proposed a more detailed kinetic scheme consisting of ten reactions. There were two new aspects in their study that are worthy of attention, the cross-reaction of the M and CM intermediates to form DMC (step R4 in [7]) and the fact that the reaction is assumed to occur on two different Cu centers, like the reactions of M or CM intermediates only between one another in pairs according to the Romano scheme [4]. Furthermore, the scheme includes the formation of the byproduct formaldehyde in the adsorbed state (step R5), whereas all the other byproducts are formed in the gas phase (steps R7–R9 in [7]).

The results obtained by the Bell's group [2, 10, 13, 19–21] show that the choice of zeolite structure is important for the carbonylation reaction [10], in particular, frameworks with a higher silica ratio (ZSM-5, MOR) better suit for the synthesis of DMM rather than DMC; for the latter, zeolites X and Y are preferred. Moreover, of zeolites with the same framework type (faujasite), the one with a higher ratio (Y) is preferable for the DMC synthesis [19], indicating a sophisticated dependence on the zeolite silica ratio. In 2008, Bell et al. replaced the scheme proposed in [7] for the formation and reactions of M or CM intermediates by a two-stage reaction of DMC formation through monomethyl carbonate (MMC) on a single cationic  $\text{Cu}^+$  center [10]. It should be noted that the formation of MMC in the hydrolysis of DMC was assumed by King [9]. It is this reaction that likely formed the basis for the mechanism of DMC formation through MMC proposed later by Zhang and Bell [10].

The data reported by Zhang and Bell [10] lead to the conclusion that along with the suggested oxida-

tion of methanol to the methoxy intermediate by adsorbed  $\text{O}_2$ , there should be a strong oxidant for the conversion of CO to  $\text{CO}_2$  via the Mars–van Krevelen redox mechanism in the absence of  $\text{O}_2$  in the gas phase. This conclusion is evident from a relatively high rate of  $\text{CO}_2$  formation by the oxidation of CO in the absence of  $\text{O}_2$  [10]. The  $\text{CO}_2$  formation rate at this CO feeding stage ( $>10^{-5}$  au) [10] is much higher than that observed in the oxidation of  $\text{CH}_3\text{OH}$  with  $\text{O}_2$  in the gas phase at the first step ( $\sim 10^{-6}$  au [10]). This rate is also higher than in the last stage ( $\sim 10^{-5}$  au) in the presence of all the reactants (“ $\text{CH}_3\text{OH}/\text{CO}/\text{O}_2$ ” step [10]), indicating a higher effectiveness of the oxidant compared with  $\text{O}_2$ . If methanol is oxidized with adsorbed oxygen alone in the Bell form involving the subsequent reaction with CO, it remains unclear which centers take part in the oxidation of CO to  $\text{CO}_2$ . The assumption on the participation of extra-framework entities, such as  $\text{CuO}_x$  for example, was made later in studies by researchers from the University of Rostock [11, 22], who used  $^{18}\text{O}_2$  leaking-in [22]. Variation of the isotopic composition of the gas revealed the involvement of  $^{16}\text{O}$  oxygen, previously trapped by the framework, as oxidant according to the Mars–van Krevelen model [22]. The experiment showed an extremely small proportion of  $\text{C}^{18}\text{O}^{16}\text{O}$  relative to that of  $\text{C}^{16}\text{O}_2$  in the CO oxidation products [22]. A quantitative difference in the progress of the DMC formation reaction in the absence of  $\text{O}_2$  in the gas phase can be seen from data published quite recently [11] or even earlier [9].

Not only single ions, but also binuclear clusters of the  $\text{Cu}_2\text{O}_x$  type and, possibly, polynuclear clusters  $\text{Cu}_n\text{O}_x$ , where  $n > 2$ , can play an important role in the explanation of the oxidative power of zeolites with copper cations. In the case of the reaction over the copper forms of zeolites, the oxidation of methane on  $\text{Cu}_2\text{O}$  clusters is an experimentally established [23, 24] and theoretically substantiated [24] fact. Our theoretical estimates made in this study confirm the oxidation of CO on  $\text{Cu}_2\text{O}_2$  clusters [25], the process that was earlier modeled on alkaline earth metal clusters [26–30]. According to our preliminary data, all the basic features inherent in alkaline earth metal carbonates (primarily, stability) are manifested in the case of copper carbonates as well, although with some differences.

Raab et al. [6] studied in more detail the involvement of extra-framework oxygen in terms of the model of  $\text{Cu}(\text{OCH}_3)_2\text{Cu}$  binuclear clusters, which can be obtained from  $\text{CuOCu}$  or  $\text{CuO}_2\text{Cu}$ . A cycle including a change in the oxidation state of copper  $\text{Cu}^{+2}/\text{Cu}^+$  at different stages was proposed. Note that regarding the evolution of the previous hypotheses, Raab et al. [6] also developed the idea of the formation of DMC via the reaction between the M and CM intermediates bound by two different copper  $\text{Cu}^{+2}$  cations, as had been suggested previously [4, 9]. It is quite likely that different mechanisms dominate at different copper concentrations. The formation of binuclear clusters and the influence of the relevant processes are more

**Table 1.** Energies (eV) of the reactants and products of the methanol reaction with MeCO<sub>3</sub>Me in mordenite (Cu-MOR) and on the 8R (2Al) cluster relative to the sum of energies of noninteracting components (methanol and carbonate in the given system) at the B3LYP (or MP2)/6-31G\* as calculated using the GAUSSIAN09 code [40] for 8R and PBE/PAW with the VASP5.3 code [41] for CuMOR. For designation of steps, see Fig. 1

Step	Me = Cu		Me = Ca	
	MOR	8R	MOR	8R <sup>a)</sup>
a1	-0.59	-0.84	-0.86	-1.33/-1.31
ts0	—	-0.20	—	-/-
a	0.13	-0.21	-0.54	-/-0.47
ts1	1.35	1.48	—	3.19 <sup>b)</sup> /-
e	0.41	0.22	0.72	0.34/0.15
ts2	0.74	0.71	—	-/-
b	0.48	-0.28	-0.05	-0.47/-0.56

a) Energy according to B3LYP/MP2 with the basis set 6-31G\*.

b) Transition state energy for C–O bond dissociation in methanol.

likely with a high copper content. The lower limit of the concentration region in which copper clusters seem to be already active, can be estimated at 8 wt % on the basis of closeness of IR spectra of the products of the DMC formation reaction on CuY samples with copper loadings of 8.22 and 15.96 wt % [11].

Numerous experimental data were considered in few theoretical studies [21, 31–33] using the schemes involving the M intermediates [21, 31] and CM inter-

mediates [32, 33]. As far as the one-center mechanism with M intermediates is concerned, there have been two theoretical studies [21, 31] using the model of an individual cluster isolated as a 6R-ring closed by OH groups from CuY. The reaction center of the 6R-ring [21] contains two Al and one Cu<sup>+</sup> cation and is an untypical center, being in a situation suitable for the doubly charged cation. The proton that counterbalances the charge of second aluminum is taken out to one of the OH groups (to form a water molecule instead of OH). Although the center was isolated from CuY, the geometry of the Cu<sup>+</sup> position in the reagent does not meet the EXAFS experimental data for CuY (Table 4 in [19]). The thermodynamics of the reactions involving consecutive attacks of two methanol molecules at the (CH<sub>3</sub>O)(OH)\* center and the formation of (CH<sub>3</sub>O)<sub>2</sub>\* was evaluated. The activation energy was determined from rate equations for the step of CO capture (using the experimental value of TOF), rather than from the results of quantum-chemical simulation. In this system, it was possible to obtain the activation energy close to the experimental value in the rate-limiting step, the insertion of CO according to the rate equations. The way of inclusion of molecular oxygen, which is to oxidize the adsorbed methanol to form the (OH)Cu(OCH<sub>3</sub>) group, was not substantiated.

In another theoretical paper [31] on this issue with the M intermediates, its authors managed to obtain, as a result of quantum-chemical simulation, the activation barrier of the inclusion of CO without creating an artificial situation with one Cu<sup>+</sup> cation on two Al centers. The cited authors also examined the dissociation

**Table 2.** Geometric parameters (Å) of the complex during the reaction by steps a–ts1–e–ts2–b

Parameter	a	ts1	e	ts2	b
C5-O103	1.280	1.422	1.477	3.280	2.824
C5-O104	1.323	1.376	1.429	1.279	1.287
C5-O105	1.275	1.304	1.334	1.275	1.277
C5-O106	3.466	1.601	1.384	1.327	1.316
C6-O106	1.417	1.446	1.445	1.459	1.453
Cu155-O105	1.903	1.900	1.875	1.852	1.875
Cu155-O104	2.148	2.054	1.990	2.816	2.603
Cu156-O104	2.010	1.999	1.988	1.912	1.915
Cu156-O103	1.959	1.937	2.012	1.799	1.819
Cu156-O103	4.623	3.243	3.313	3.194	2.997
O106-O105	3.536	2.439	2.32	2.250	2.277
O104-O105	2.207	2.209	2.188	2.227	2.219
H1-O103	1.932	1.249	0.981	0.979	0.982
H1-O106	0.979	1.242	2.150	1.976	3.872
Cu156-O104-Cu155	156.04	139.67	135.05	157.8	149.34
Cu156-O103-H1	146.47	111.44	117.04	112.48	109.54
C5-O106-H1	43.82	71.88	65.13	111.9	73.89

**Table 3.** Activation barriers (eV) and imaginary frequencies ( $\text{cm}^{-1}$ ) of reaction steps in the first stage of methanol carbonylation according to results of QST3 calculation at the B3LYP/6-31G\* level

Step	$-i\omega$	$\Delta E$
a1-a	21.3	0.82
a-e <sup>a)</sup>	1369.1	1.48
a-e	1628.9	1.69
e-b <sup>a)</sup>	98.2	0.33
e-b	324.4	0.49
e-b <sup>b)</sup>	595.3	3.19

a) In mordenite by PBE/PAW calculation with the NEB method.

b) Transition state energy for C–O bond dissociation in methanol.

of  $\text{O}_2$  on a pair of copper atoms in the channel of  $\text{Cu}\beta$  zeolite, but the resulting barrier of 1.71 eV turned to be larger than the critical one for the inclusion of CO (0.65 eV) and, therefore, it is inconsistent with the experimental data, since the stage of formation of two  $>\text{Cu}=\text{O}$  pairs from  $\text{O}_2$  is a rate-limiting step instead of the CO capture stage. As a factor justifying the dissociation of  $\text{O}_2$  with a barrier of 1.71 eV, a large amount of energy received by the system in the form of heat of the exothermic reaction (1.84 eV) at the previous  $\text{O}_2$  capture step is considered in [31], although the possibility to accumulate the effect on the relevant reaction coordinate (essentially, on the O–O bond) was not explained. Unfortunately, the  $\text{O}_2$  dissociation step was considered on the  $\text{Cu}\beta$  zeolite [31], for which there is no experimental data on the carbonylation of alcohols. A common problem of discussing  $\text{O}_2$  dissociation processes within the generalized gradient approximation (GGA) of the density functional theory (DFT) or the hybrid (DFT/B3LYP) approach has been addressed in our recent paper [34]. The problem is related to the inversion of relative energies of the singlet and triplet states of  $\text{CuO}_x\text{Cu}$  clusters,  $X = 1$  or  $2$ , in terms of the DFT/GGA and DFT/B3LYP approximations compared with their ratio according to MP2/6-31G\* calculation [34]. This inversion makes it possible to consider individually different spin states, not the transitions between them that inevitably occur during the dissociation of triplet  $\text{O}_2$ . The geometry of position of  $\text{Cu}^{+1}$  was optimized in the reactant on the same 6R-fragment of zeolite and is consistent with EXAFS experimental data assuming the cation coordination of 2.7 obtained for another zeolite  $\text{CuZSM-5}$  [35]. The activation energy of the individual steps was determined using linear transition-state (TS) search algorithms that require correction by the intrinsic reaction coordinate or the nudged elastic band (NEB) method.

The second mechanism with the CM intermediates proceeds from the ease of methanol dissociation and formation of methoxy groups. This assumption is easy

to substantiate by calculation for  $\text{Cu}^{+2}$  when there are two Al atoms in the moiety, so that the proton can move to the second oxygen atom of the Si–O–Al group, but it is not obvious for  $\text{Cu}^{+}$  located near the single Al atom. In the case of  $\text{Cu}^{+}$ , this reaction should be accompanied by the “kinetic” stabilization of the products when the proton has time to migrate to the remote center ( $>5 \text{ \AA}$ ), impeding the recombination of methanol [36, 37]. According to this scheme, the attack of CO at the methoxy group results in the formation of the carbomethoxy intermediate. It participates in the reaction with the second methanol molecule in the next step. Both of the theoretical studies based on this concept of the mechanism and more representative models (30T or 31T) of isolated cluster resulted in reasonable values of the activation energy of about 15 kcal/mol [32, 33]. At the same time, our more recent calculations [25] of the activation barriers by different TS search methods (QST3, NEB) and versions of DFT approximation (HSEh1PBE, B3LYP, wB97XD, PBE) showed significantly lower activation barriers (1.18–10.44 kcal/mol with cluster models and 4.00–9.11 kcal/mol with allowance for periodic boundary conditions in CuMOR) than those calculated with the LST algorithm [32, 33] or observed experimentally [10, 20]; a systematic difference between the calculated spectra of the CM intermediates and the spectrum observed in [9, 10] was also shown. At the same time, the geometry and spectra of the reactants in the formation of the CM intermediates were calculated in our study [25] in good agreement with the experiment [19], and the transition state frequencies and the heat of reactions are close to those obtained in [32, 33]. Therefore, the solution [32, 33] in favor of the mechanism through the CM intermediates cannot be considered definitive.

The problem for both types of mechanism (M and CM intermediates) is the substantiation of the redox scheme of the process involving the oxygen capture and the change in the oxidation state of copper. Experimental data obtained by the Bell's group [10] and the group from the University of Rostock [11, 22] show that the case of CO feeding without oxygen (but preliminary feeding with a  $\text{CH}_3\text{OH}/\text{O}_2$  mixture and removing in a He stream of all weakly adsorbed species), the reaction continues with a lower yield. This oxygen can participate in the form of the known one-center ( $\text{CuO}_X$ ); two-center  $\text{CuO}_x\text{Cu}$ ,  $x = 1$  or  $2$ ; and  $\text{CuCO}_3\text{Cu}$  entities or new formations. The first compound of this series for the manufacturing of DMC via the reaction with CO was  $\text{Cu}(\text{OCH}_3)_2\text{Cu}$  proposed by Saegusa et al. [2], but the mechanism of this reaction was not theoretically studied. Experimental data obtained by Engeldinger and others [11, 22] showed the formation of formates, whose IR spectra are similar to the spectra of carbonates. It is likely that the  $\text{CuO}_2\text{Cu}$  cluster can oxidize CO to  $\text{CuCO}_3\text{Cu}$ , whose activity can also be assessed in the reaction with methanol. Formally, carbonate can be formed on one cat-

ion as well, more likely, in the form of hydrogen carbonate and then participate in the reaction.

Inertness of  $\text{CO}_2$  is a significant obstacle, and its conversion into the carbonate form in the zeolite may be a better solution to improve reactivity. Engeldinger et al. [11] noted the involvement of framework oxygen in the form of  $\text{CuO}_x$ , however, the participation of the binuclear cluster  $\text{CuO}_x\text{Cu}$ ,  $x = 1$  or  $2$ , is more likely [23, 24]. In [26], we have shown that the alkaline earth metal species  $\text{MeO}_x\text{Me}$ ,  $x = 1-4$ , with higher oxygen content ( $x > 2$ ) are involved in the barrier-free formation of a  $\text{MeCO}_3\text{Me}$  carbonate with alkaline earth metal cations. Later, these conclusions were found to be valid for  $\text{CuO}_2\text{Cu}$  as well [25]. What is unusual compared with alkaline earth metal carbonates is the aforementioned peak intensity ratio of 20 : 1 of symmetric ( $1399.4 \text{ cm}^{-1}$ ) to asymmetric ( $1626.6 \text{ cm}^{-1}$ )  $\text{CuCO}_3\text{Cu}$  vibrations at the same calculation level B3LYP/6-31G\* [25], which results in close intensities of both bands for alkaline earth metal carbonates [26, 30] and qualitative agreement with the experiment [40]. This  $\text{CuO}_2\text{Cu}$  cluster can be a source of oxygen for  $\text{CO}_2$  conversion into carbonate, which we have shown in [26, 30], despite the fact that neither our theoretical attempts [26] nor the work by other investigators [39] confirm the carbonate formation involving framework oxygen atoms.

Let us summarize the results of this brief review. The conventional scheme of oxidative carbonylation consists of two steps to form copper methoxide in the first step [4, 9] followed by conversion into copper monomethyl carbonate [10] or the carbomethoxy intermediate [3, 4, 9] in the attack of the first  $\text{CH}_3\text{OH}$  molecule. In the second step, the products of the first step react with  $\text{CO}$ . As a result, the mechanism cannot be considered completely elucidated and the nature of intermediate products in favor of monomethyl carbonate [10] or copper carbomethoxide [9] remains an open question. It should be added that formaldehyde suggested to form in [9, 10] was not detected spectroscopically (in any of the cited papers) or chromatographically [11], a fact that may be due to its rapid conversion to methyl formate or deep oxidation to  $\text{CO}_2$ .

The carbonate can be formed under the conventional DMC synthesis conditions in the oxidation of  $\text{CO}$  on the  $\text{CuO}_2\text{Cu}$  cluster. We examined the existence of such a step using the approach with periodic boundary conditions (PBC) in the zeolite CuMOR and found the barrier to be about 1 eV in the first choice of the  $\text{CuO}_2\text{Cu}$  position over a fragment of the 8R window on the “bottom” of the main channel of CuMOR [25]. This energy is higher than that required for other zeolites, for which experimental data are available. But we assume that this value varies between the forms and the energy can be lower in the case of more detailed optimization of the  $\text{CuO}_2\text{Cu}$  location in the initial position. It is important that frequency splitting of symmetric and asymmetric vibrations in the

carbonate ( $227.2 \text{ cm}^{-1} = 1626.6-1399.4 \text{ cm}^{-1}$ , see above) [25] is in good agreement with the values measured experimentally ( $226 \text{ cm}^{-1}$  [11]  $221 \text{ cm}^{-1}$  [22]) and attributed earlier to the formate. In this paper, we consider the “carbonate” mechanism of oxidative carbonylation of methanol through its attack on  $\text{CuCO}_3\text{Cu}$ .

## CALCULATION PROCEDURE

Two types of models were used, the isolated cluster model calculated with the software code GAUSSIAN09 [40] and the model with PBCs calculated using the VASP5.3 code [41]. The model of  $\text{CuCO}_3\text{Cu}$  carbonate chemisorbed on the single 8R cluster containing two Al atoms was analyzed at the level of the hybrid density functional theory (DFT/B3LYP/6-31G\*) and the Møller–Plesset post-Hartree–Fock second-order perturbation theory (MP2/6-31G\*) and that in the zeolite CuMOR (also two Al atoms per cell), at the PBE/PAW level. The transition state (TS) parameters were calculated using the QST3 method [40] for the cluster models and the NEB method [42, 43] for the models with PBCs.

## RESULTS AND ITS DISCUSSION

Consider the first step of the methanol attack on the carbonate formed in zeolites. It should be noted that the carbonates are produced by the reaction in zeolites of metal oxide  $\text{MeO}_x\text{Me}$  clusters,  $x = 1-4$ , with  $\text{CO}_2$  or  $\text{CO}$ , which is easily oxidized to  $\text{CO}_2$  on them as on the Zn- or Mg-forms or to carbonates as on other alkaline earth forms [26–30]. Studying the reaction of carbonates with methanol, we examined elementary steps involving intermediates “a”, “e”, and “b” (Fig. 1) and a set of transition states on the Cu-form at different levels of the theory, including approaches with periodic boundary conditions. The intermediates on the Ca-form were also described (Table 1).

It was shown that the limiting step on the Cu-form is step “a–e” of proton transfer from methanol to intermediate “e” with an activation energy of 1.48 eV (with periodic boundary conditions) to 1.69 eV (single 8R-cluster). A reasonable value for the barrier was obtained owing intermediate state “a”, which can be reached by overcoming a smaller barrier of 0.64 eV (8R-cluster) from the deepest minimum “a1”, the geometry of which is not very different between the 8R cluster (Fig. 1) and the MOR framework. The reaction coordinate along a very gentle barrier between states “a1” and “a” ( $\omega = 21.3i \text{ cm}^{-1}$ ) corresponds to the rotation of the methanol molecule as a whole. This transition state (TS) ts0 could be described only in the approximation of the single 8R-cluster. The angle formed by the methanol neighboring copper atom, oxygen atom  $\text{O}_{cl}$  located between the copper atoms of the cluster, and methanol oxygen atom  $\text{O}_m$  increases

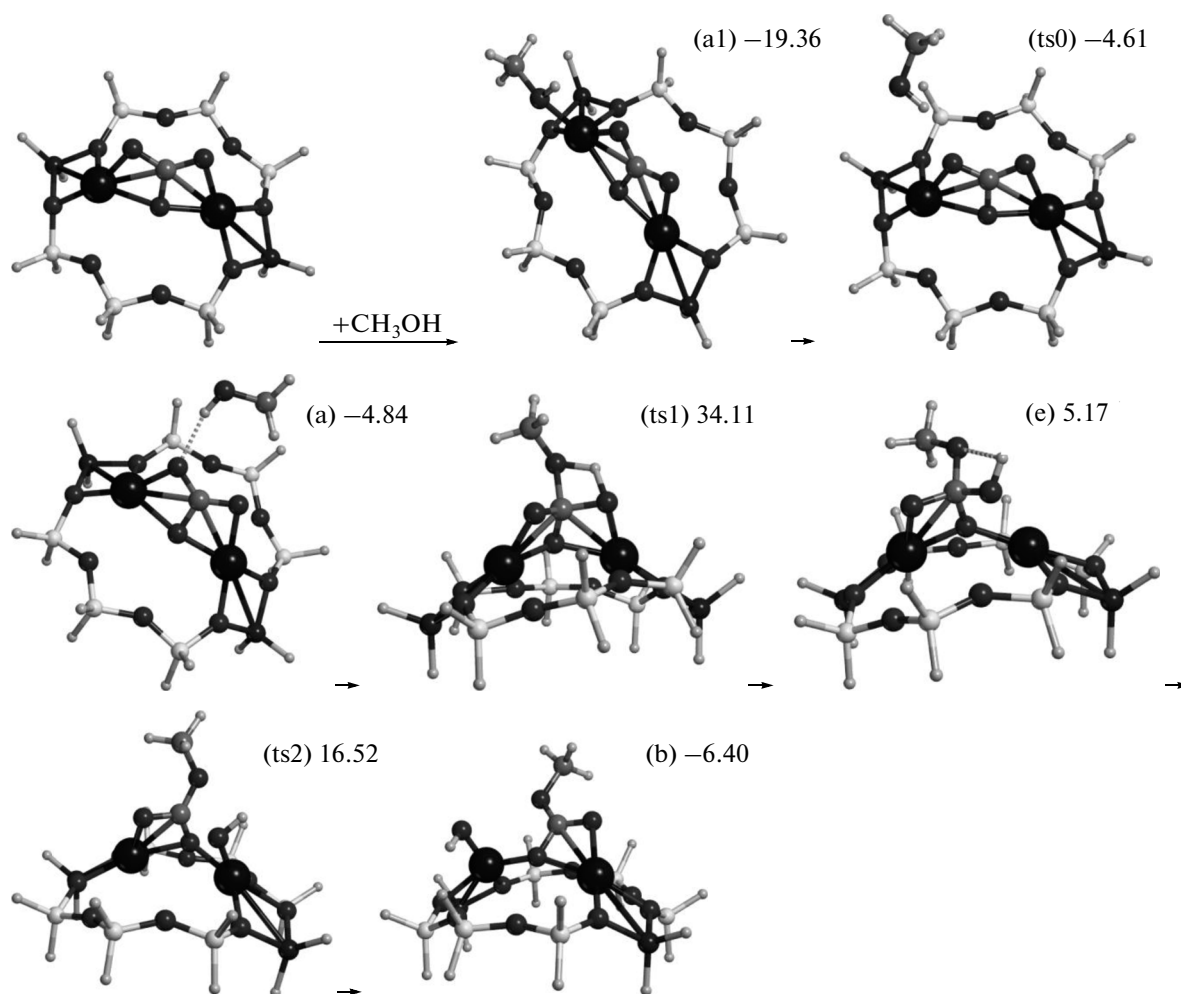


**Fig. 1.** The first stage of the catalytic process of methanol carbonylation on copper carbonate, which is formed in the 8R ring of mordenite. Steps are labeled, starting with (a1) to (b); here, the energies (kcal/mol) are given relative to the sum of the energies of noninteracting carbonate and methanol; in Table 1, they are given in eV to compare with the quantities for the model of the process in CuMOR.

in the order a1 ( $\angle\text{Cu}-\text{O}_{\text{cl}}-\text{O}_{\text{m}} = 22.37^\circ$ )  $\rightarrow$  ts0 ( $49.49^\circ$ )  $\rightarrow$  a ( $70.59^\circ$ ). Upon movement in this order, methanol changes its position relative to the carbonate plane in the first step a1  $\rightarrow$  ts0, so that it occurs almost in the carbonate plane at step “a.” The same character of methanol movement relative to the carbonate plane is conserved in the case of MP2 calculation. In the latter case, however, the deviation of cations from the carbonate plane increases.

The main reaction involving a change of the carbon atom hybridization occurs from state “a”: a( $sp^2$ )  $\rightarrow$  e( $sp^3$ )  $\rightarrow$  b( $sp^2$ ). Stabilization of all intermediates is more pronounced in the cluster model (Table 1) than in CuMOR. The same is true for a similar series of Ca intermediates and, to an even greater extent, on the MP2 level than in the DFT/GGA calculation. Evolution of the geometry of Cu intermediates during the process is shown in Table 2. In the case of CaMOR, we failed to calculate the geometry of the transition state. A large imaginary frequency of proton transfer

between the oxygen atoms bound to the carbon atom is not varied much in step “a–e” by changing the calculation method (Table 1). The corresponding highest reaction barrier of 1.69 eV in the cluster model is reduced to 1.48 eV (or by 12.4%) in the approximation with periodic boundary conditions (PBCs), a change that can be partly attributed to the influence of electrostatic field in CuMOR pores. This opens the possibility of further searching for appropriate zeolite frameworks to achieve the minimum activation barrier.

The parameters of all transition states revealed by various methods are shown in Table 3. Note that in both cases “ts1” and “ts2”, the barrier values and frequencies values calculated with PBCs in the CuMOR structure are less than those in the case of 8R cluster.

Figure 2 shows the geometry of the complex during the reaction via steps a–ts1–e–ts2–b, as calculated for the CuMOR model at the PBE/PAW level. It is seen in the figure that an additional difference in the

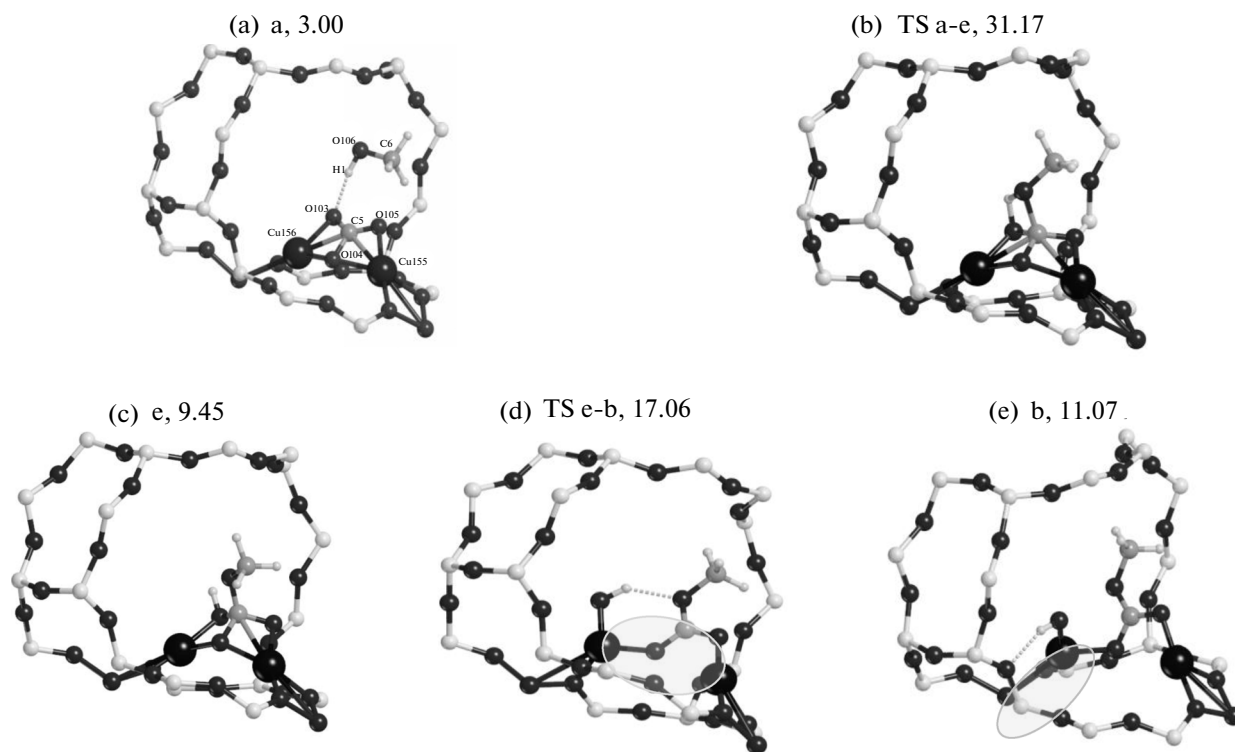


**Fig. 2.** Geometry of the complex during reaction proceeding by steps a—ts1—e—ts2—b, as calculated for the CuMOR model at the PBE/PAW level. The ellipse shows the region of the hydrogen bond that appears only in the version of calculation with PBCs. The notation of atoms (a) of the complex is the same as in Table 2. The relative energy is given in kcal/mol.

“ts2” profile along the reaction coordinate is the appearance of a small minimum given by calculation with PBCs, which is due to the introduction of a hydrogen bond (shown by the ellipse in Fig. 2d) that is not included in the cluster model (Fig. 1, case b) because of a different orientation of the proton. However, neither this hydrogen bond nor the one formed with framework oxygen (Fig. 2e) leads to better stabilization of state “b” in the calculation with PBCs. The failure to enhance stabilization can be explained as a consequence of a greater extension of the complex along the MOR canal, which we reported for stretching of the entire 8R fragment of MOR in the solution with PBCs concerning the dissociation of water [36]. The Cu···Cu and Al···Al distances are shorter in the MOR model (8.361 and 8.544 Å) than in the 8R-cluster model (8.117 and 8.289 Å).

In summary, the literature on the known schemes of oxidative carbonylation of methanol, including methoxy intermediates, carbomethoxy intermediates, carbonates, and Cu(OCH<sub>3</sub>)<sub>2</sub>Cu binuclear clusters has been analyzed. We investigated the rate-limiting step of methanol molecule attack on copper carbonate in the single cluster (8R type) model at the density functional theory (DFT) and Møller–Plesset (MP2) levels and the model with periodic boundary conditions (PBCs) on CuMOR zeolite at the PBE/PAW level. The calculated value of the barrier on CuMOR is more

than two times greater than the known values to be 11.70 or 14.80 kcal/mol for CuZSM-5 [35] or CuY [10], respectively, indicating inadequate description of the process in which the rate-limiting step according to the experimental data should be the insertion of CO. These barriers are higher than the activation energy at the CO inclusion step (found earlier as 23.94 kcal/mol for CO on Cu<sub>2</sub>O<sub>2</sub> in the calculation with PBCs [25]), which should be maximal relative to that in all the other steps. This discrepancy, of course, cannot be considered to completely discriminate the mechanism.

As the next step of investigation, it is reasonable to search for a less strongly coordinated carbonate particle as an active center with the varying position of Al atoms in the lattice.

#### ACKNOWLEDGMENTS

The work was supported by the Russian Foundation for Basic Research, project no. 12-03-00749-a.

The authors are grateful to the Lomonosov Supercomputer Complex for providing the computer time [44].

#### REFERENCES

1. T. Saegusa, T. Tsuda, K. Isayama, and K. Nishijima, *Tetrahedron Lett.* **9**, 831 (1968).

2. T. Saegusa, T. Tsuda, and K. Isayama, *Org. Chem.* **35**, 2976 (1970).
3. P. Koch, G. Cipriani, and E. Perrotti, *Gazz. Chim. Ital.* **104**, 599 (1974).
4. U. Romano, R. Tesel, M. M. Mauri, and P. Rebora, *Ind. Eng. Chem. Res.* **19**, 396 (1980).
5. W. Mo, H. Xiong, J. Hu, Y. Ni, G. Li, *Appl. Organomet. Chem.* **24**, 576 (2010).
6. V. Raab, M. Merz, and J. Sundermeyer, *J. Mol. Catal. A: Chem.* **175**, 51 (2001).
7. S. A. Anderson and T. W. Root, *J. Catal.* **217**, 396 (2003).
8. S. A. Anderson and T. W. Root, *J. Mol. Catal. A: Chem.* **220**, 247 (2004).
9. S. T. King, *J. Catal.* **161**, 530 (1996).
10. Y. Zhang and A. T. Bell, *J. Catal.* **255**, 153 (2008).
11. J. Engeldinger, C. Domke, M. Richter, and U. Bentrup, *Appl. Catal., A* **382**, 303 (2010).
12. G. Rebmann, V. Keller, M. J. Ledoux, and N. Keller, *Green Chem.* **10**, 207 (2008).
13. Y. Zhang, D. Briggs, E. de Smitt, and A. T. Bell, *J. Catal.* **251**, 443 (2007).
14. N. Keller, G. Rebmann, and V. Keller, *J. Mol. Catal. A: Chem.* **317**, 1 (2010).
15. T. Sakakura, J. -C. Choi, and H. Yasuda, *Chem. Rev.* **107**, 2365 (2007).
16. E. Leino, P. Maki-Arvela, V. Eta, et al., *Appl. Catal., A* **383**, 1 (2010).
17. N. Kitajima and Y. Moro-oka, *Chem. Rev.* **94**, 737 (1994).
18. W. B. Tolman, *Acc. Chem. Res.* **30**, 227 (1997).
19. I. J. Drake, Y. Zhang, D. Briggs, et al., *J. Phys. Chem. B* **110**, 11654 (2006).
20. Y. Zhang, I. Drake, D. Briggs, and A. T. Bell, *J. Catal.* **244**, 219 (2006).
21. X. Zheng and A. T. Bell, *J. Phys. Chem. C* **112**, 5043 (2008).
22. J. Engeldinger, M. Richter, and U. Bentrup, *Phys. Chem. Chem. Phys.* **14**, 2183 (2012).
23. M. H. Groothaert, P. J. Smeets, B. F. Sels, et al., *J. Am. Chem. Soc.* **127**, 1394 (2005).
24. J. S. Woertink, P. J. Smeets, M. H. Groothaert, et al., *Proc. Natl. Acad. Sci. USA* **106**, 18908 (2009).
25. A. A. Rybakov, A. V. Larin, and G. M. Zhidomirov, *Comput. Theor. Chem.* (submitted), No. COMPTC-D-15-01017.
26. A. V. Larin, A. A. Rybakov, G. M. Zhidomirov, et al., *J. Catal.* **281**, 212 (2011).
27. G. M. Zhidomirov, A. V. Larin, D. N. Trubnikov, and D. P. Vercauteren, *J. Phys. Chem. C* **113**, 8258 (2009).
28. A. V. Larin, G. M. Zhidomirov, D. N. Trubnikov, and D. P. Vercauteren, *J. Comput. Chem.* **31**, 421 (2010).
29. A. A. Rybakov, A. V. Larin, G. M. Zhidomirov, et al., *Comput. Theor. Chem.* **964**, 108 (2011).
30. G. M. Zhidomirov, A. A. Shubin, A. V. Larin, et al., *Practical Aspects of Computational Chemistry: I. An Overview of the Last Two Decades and Current Trends*, Ed. by J. Leszczynski and M. K. Shukla (Springer, Dordrecht, 2012), p. 579.
31. Y. Shen, Q. Meng, S. Huang, et al., *RSC Adv.* **2**, 7109 (2012).
32. R. Zhang, J. Li, and B. Wang, *RSC Adv.* **3**, 12287 (2013).
33. H. Zheng, J. Qi, R. Zhang, et al., *Fuel Process. Technol.* **128**, 310 (2014).
34. A. A. Rybakov, I. A. Bryukhanov, A. V. Larin, and G. M. Zhidomirov, *Int. J. Quantum Chem.* **115**, 1709 (2015).
35. I. J. Drake, Y. Zhang, M. K. Gilles, et al., *J. Phys. Chem. B* **110**, 11665 (2006).
36. A. V. Larin, A. A. Rybakov, and G. M. Zhidomirov, *J. Phys. Chem. C* **116**, 2399 (2012).
37. A. A. Rybakov, A. V. Larin, and G. M. Zhidomirov, *Inorg. Chem.* **51**, 12165 (2012).
38. J. W. Ward and H. W. Habgood, *J. Phys. Chem.* **70**, 1178 (1966).
39. E. Garrone, B. Bonelli, C. Lamberti, et al., *J. Chem. Phys.* **117** (22), 10274 (2002).
40. M. J. Frisch, G. W. Trucks, H. B. Schlegel, et al., *Gaussian 09, Revision A.02*, (Gaussian, Wallingford, CT, 2009).
41. G. Kresse and J. Hafner, *Phys. Rev. B* **47**, 558 (1993).
42. G. Kresse and J. Furthmuller, *Phys. Rev. B* **54**, 11169 (1996).
43. G. Henkelman, B. P. Uberuaga, and H. Jónsson, *J. Chem. Phys.* **113**, 9901 (2000).
44. V. V. Voevodin, S. A. Zhumatii, S. I. Sobolev, et al., *Otkrytye Sistemy*, No. 7, 36 (2012).

*Translated by S. Zatonksy*